3rd URSI AT-AP-RASC, Gran Canaria, 29 May – 3 June 2022

Spatial sensor arrangement in Through-the Wall radar imaging: Numerical results

Maria Antonia Maisto* (1), Mehdi Masoodi (1), Raffaele Solimene(1)
(1) Department of Engineering University of Campania Aversa (Ce), 81031, Italy

Abstract

In this contribution, the problem to collect the scattered field data in a multi-monostatic and multi-frequency configuration is addressed in the framework of through-the wall-imaging. A numerical analysis shows that in order to collect the data with the minimal number of measurements, a non uniform sampling strategy must be exploited.

1 Introduction

The electromagnetic wave capability to penetrate within obstacles allows to detect, localize and electromagnetically characterize targets embedded within them. It is an important issue in different branches of remote sensing for example, in the framework of ground penetrating radar (GPR) [1] or in nondestructive testing (NDT), the imaging of metallic pipes [2], biomedical imaging [3] and throw-the wall-imaging [4]. In particular , in the latter, electromagnetic wave signals are transmitted and collected throw a wall at several locations, in order to imaging a target located beyond it. Many papers in literature are devoted to introduce new reconstruction algorithms such delay-and-sum beamforming [5, 6], backprojection [7], contrast source inversion [8], and diffraction tomography (DT) [9, 10]. They aims to obtain an high quality imaging reconstruction with low computational effort and high precessing speed. For all considered algorithms, high range and cross-range resolutions are achieved by using ultra-wideband (UWB) signals and antenna arrays with large apertures, respectively [11]. This means that in order to improve resolution, long arrays and UWB signals are generally demanded, which results in a long time for data collection, a huge amount of data, and a high computational complexity. As the data collection time prolongs, the targets may change positions, and their movements may cause smearing and blurring in the processed image. Moreover, the most acquisition time is spent on the antenna displacement rather than the frequency sweeps . Accordingly, in this paper a strategy to collect the spatial data which allows to minimize the number of measurements without affecting the performance achievable in the reconstruction is introduced in the framework of TWRI . In other words, the new sampling strategy returns a number of data close to the Number od Degree of Freedom (NDF) [12] without reducing the information content of the field [13]. The proposed approach is inspired by [14] and [15] where the new sampling scheme is devised as to one which allows to approximate the ideal point-spread function, that is the one obtained in the case where data are continuously collected over the measurement domain. A numerical analysis shows that the spatial measurements must be nonuniformly arranged across the measurement domain according to a law which depends on geometrical parameters, in particular on the wall parameters. A numerical examples shows the good results obtained by exploiting this collection strategy.

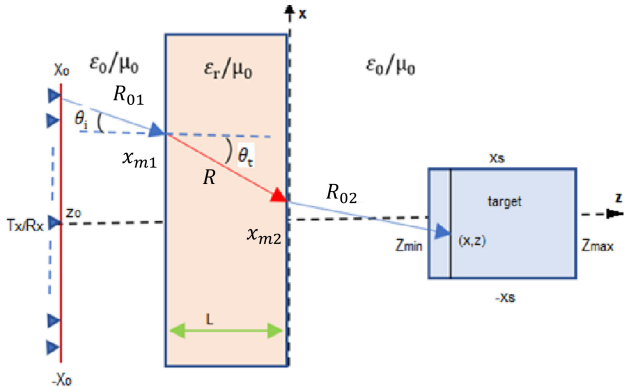

Figure 1. Geometry of the problem

2 Scattering model

Consider the geometry sketched in Fig. (1). The wall is schematized as a three-layer medium (air-wall-air). The targets are assumed to reside within the rectangular region $SD = [-X_s, X_s] \times [z_{min}, z_{max}]$ and they are embedded within the third layer. The incident field is radiated by y-polarized line source of unitary amplitude at different frequencies, with the wavenumber k_0 which varies in a band $\Omega_k = [k_{min}, k_{max}]$. The wall thickness and permittivity L and ε_r are known. In order to collect the data, a monostotic configuration is considered where the transmitting and receiving antenna move together along the segment $OD = [-X_o, X_o]$ placed at z_o in the first layer. Under the Born approximation the scattered field E_s is given by

$$E(x_o, k_0) = jk_0^2 \omega \mu_0 \int_{SD} G^2(x_o, \boldsymbol{r}, k_0) \chi(\boldsymbol{r}) d\boldsymbol{r} \qquad (1)$$

with $(x_o, k_0) \in \Omega_k \times OD$ and $\boldsymbol{r} = (x, z)$. The function $\chi(\boldsymbol{r}) = (\varepsilon_s(\boldsymbol{r}) - \varepsilon_0)/\varepsilon_0$ is the so-called contrast function, with ε_s being the dielectric permittivity of the unknown scatterer,

accounting for the relative difference between the background and target electromagnetic parameters. The function $G(x_o, \boldsymbol{r}, k_0)$ is the Green function accounting for three layered background medium whose spectral representation is

$$G(x_o, \boldsymbol{r}, k_0) = \frac{-j}{4\pi} \int_{-\infty}^{\infty} T(k_x) e^{-jk_{zb}L} e^{jk_{z0}(L+z_o-z)} e^{-jk_x(x_o-x)} dk_x \tag{2}$$

with k_x the spectral variable,

$$k_{z0} = \begin{cases} \sqrt{k_0^2 - k_x^2} & \text{if} \quad k_x \leq k_0 \\ -j\sqrt{k_x^2 - k_0^2} & \text{if} \quad k_x > k_0 \end{cases}$$

$$k_{zb} = \begin{cases} \sqrt{k_b^2 - k_x^2} & \text{if} \quad k_x \leq k_b \\ -j\sqrt{k_x^2 - k_b^2} & \text{if} \quad k_x > k_b \end{cases}$$

and the transmitting coefficient $T(k_x)$ given by

$$T(k_x) = \frac{1 - \Gamma.^2}{k_{z0}(1 - \Gamma.^2 e^{-2jk_{zb}L})} \tag{3}$$

with

$$\Gamma = \frac{k_{zb} - k_{z0}}{k_{zb} + k_{z0}} \tag{4}$$

If it is assumed that $L > \frac{\lambda_{0min}}{n}$ and $z_{min} - L - z_o > \lambda_{0min}$, with λ_{0min} the free space wavelength at the maximal frequency and $n = \sqrt{\varepsilon_r}$ the refractive index, the asymptotic evaluation of the spectral representation of $G(x_o, \boldsymbol{r}, k_0)$ results into the following expression for the Green function

$$G(x_o, \boldsymbol{r}, k_0) \approx \sqrt{h(x_o, \boldsymbol{r}, k_0)} e^{-jk_0\phi(x_o, \boldsymbol{r})} \tag{5}$$

where $\sqrt{h(x_o, \boldsymbol{r}, k_0)}$ is the relevant amplitude factors, and $\phi(x_o, \boldsymbol{r}) = (R_{01} + R_{02} + nR)$ is the phase term that takes into account the three paths from the target point $\boldsymbol{r} = (x, z)$ to the field point $\boldsymbol{r}_o = (x_o, z_o)$ which the waves propagate through. In particular, $R_{01} = \sqrt{(x_{m1}(x_o, \boldsymbol{r}) - x_o)^2 + (L + z_o)^2}$, $R_{02} = \sqrt{(x - x_{m2}(x_o, \boldsymbol{r}))^2 + z^2}$ and $R = \sqrt{(x_{m2}(x_o, \boldsymbol{r}) - x_{m1}(x_o, \boldsymbol{r}))^2 + L^2}$ are the two paths travelled by the waves in free space and the one travelled by the waves in the wall, respectively. Finally, $x_{m1}(x_o, \boldsymbol{r})$ and $x_{m2}(x_o, \boldsymbol{r})$ are the refraction points which are given by the Snell's law as

$$\frac{x_{m1} - x_o}{R_{01}} = n\frac{x_{m2} - x_{m1}}{R} = \frac{x - x_{m2}}{R_{02}} \tag{6}$$

In a typical TWRI scenario, the most acquisition time is spent on the antenna displacement rather than the frequency sweeps. Accordingly, in order to reduce the acquisition time efficiently, the focus, here, is on the minimization of the spatial measurements rather than the frequencies. In order to find a sampling scheme which suggests how to collect the spatial data, the strategy developed in [14] and [15] is exploited. In those papers, the idea is to devise the new sampling scheme that allows to approximate the ideal point-spread function, that is the one obtained in the case where data are continuously collected over the measurement domain. As point-spread function, the one returned by approximating the inverse of scattering operator with its adjoint is considered. Note that this inversion strategy is very common in literature and known as migration scheme. Accordingly, the point-spread function obtained by such an inversion scheme is

$$psf(\boldsymbol{r}, \boldsymbol{r}') = \int_{\Sigma} dk_0 dx_o [k_0^2 \omega \mu_0]^2 G^2(x_o, \boldsymbol{r}', k_0) G^{2*}(x_o, \boldsymbol{r}, k_0) \tag{7}$$

with $\Sigma = \Omega_k \times OD$. Inspired by the approach developed in [14] and [15], a numerical analysis shows that the spatial measurements must be collected with an uniform step into a new variable ζ depending on the configuration parameters as

$$\zeta(x_o) = k_{max}\big[n\sqrt{(x_o - f_1)^2 + L^2} + \\ + \sqrt{(f_1 + X_s)^2 + (z_{min} - L - z_o)^2} - n\sqrt{(x_o - f_2)^2 + L^2} - \\ - \sqrt{(f_2 - X_s)^2 + (z_{min} - L - z_o)^2}\big] \tag{8}$$

where f_1 and f_2 are refraction points obtained by the Snellâ˘Źs law corresponding to extreme points in investigation domain

$$f_1 = x_{m3}(x_o, -X_s)$$
$$f_2 = x_{m3}(x_o, X_s)$$

The uniform sampling step with respect to ζ is defined as

$$\zeta(x_o) - \zeta(x_o + \Delta_{x_o}) = \frac{\pi}{\alpha} \tag{9}$$

with $\alpha = 1.1$ be an oversampling factor. The non-linear relationship between ζ and x_o results in a non-uniform sampling distribution of samples falling within OD. Hence, the required number of non-uniform spatial samples falling within OD, corresponding to the interval $[\zeta_{-X_o}, \zeta_{X_o}]$, turns to be

$$N = \frac{2k_{max}\alpha\zeta X_o}{\pi}. \tag{10}$$

3 Numerical results

In this section, in order to appreciate the good results provided by the proposed sampling scheme, the exact point spread function psf and the one obtained by the proposed sampling scheme are compared. The exact point spread function psf is evaluated numerically by implementing the (7) with a very fine and uniform grid of spatial points within OD. Instead, when the proposed non-uniform sampling strategy is considered, the point-spread function is evaluated by

$$psf_e(\boldsymbol{r}, \boldsymbol{r}') = \sum_{l=1}^{N_k} \sum_{m=1}^{N} \Delta k_0 [k_{0l}^2 \omega_l \mu_0]^2 G^2(x_{om}, \boldsymbol{r}', k_{0l}) \\ \times G^{2*}(x_{om}, \boldsymbol{r}, k_{0l}) \frac{dx_o}{d\zeta}|_{x_o = x_{om}} \Delta\zeta \tag{11}$$

where $\frac{dx_o}{d\zeta}$ is due to the change of variable from x_o to ζ, introduced in order to approximate the integral in x_o of (**??**).

Note that in order to collect the frequencies standard arguments based on the range extent of the area to be imaged are applied. They suggest to sample with an uniform step equal to $\Delta k_0 = \pi/(z_{max} - z_{min})$. Accordingly, N_k is the number of frequencies fallen within Ω_k. Suppose to set the configuration parameter as $X_s = 0.7m$, $z_{min} = 0.2m$, $z_{max} = 1.2m$, $k_{min} = 6.67\pi m^{-1}$, $k_{max} = 10.67\pi m^{-1}$, $X_0 = 1m$, $z_o = -0.5m$, $d = 20cm$ and $n = 3$ and the source position is $\boldsymbol{r}' = (0.5, 0.5)m$. The corresponding normalized point-spread functions are shown in Fig. 2. In this figure, it is shown: the normalized psf and the spatial sampling strategy exploited to achieve its estimation (panel a); the normalized psf_e and the non uniform spatial sampling strategy exploited to achieve its estimation (panel b); the cut-views along x and z, in particular the blue and red lines refer psf and psf_e, respectively. As can be seen , psf and psf_e practically always overlap. This means that the proposed spatial sampling strategy works very well for estimating the point spread function regardless the wall parameters.

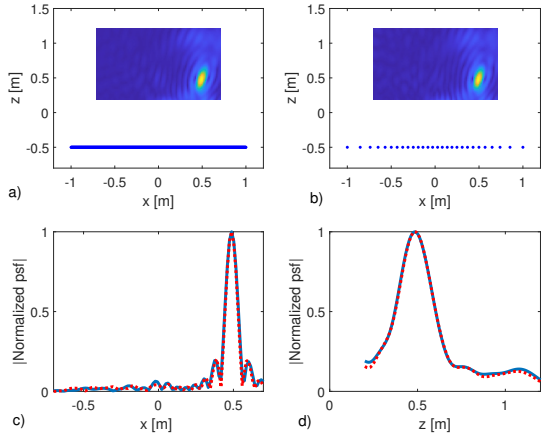

Figure 2. Illustrating the normalized point-spread function amplitudes. The configuration parameters are $X_s = 0.7m$, $z_{min} = 0.2m$, $z_{max} = 1.2m$, $k_{min} = 6.67\pi m^{-1}$, $k_{max} = 10.67\pi m^{-1}$, $X_0 = 1m$, $z_o = -0.5m$, $d = 20cm$ and $n = 3$. The source position is $\boldsymbol{r}' = (0.5, 0.5)m$. Panel a) shows the normalized psf and the spatial sampling strategy exploited to achieve its estimation; panel b) the normalized psf_e and the non uniform spatial sampling strategy exploited to achieve its estimation; panel c) and d) the cut-views along x and z, in particular the blue and red lines refer psf and psf_e, respectively. $N = 28$.

4 Conclusion

In this paper, a strategy to collect the scattered field data in spatial position in the framework of through-the wall radar imaging has been proposed. This strategy leads to a non uniform sampling scheme that is typical for near field configuration and has already been observed for homogeneous case. However, compared homogeneous case, the way in which the number of sampling points and their non-uniform distribution is affected by the configuration parameters is different. In particular, they are affected by the wall parameters.

References

[1] R. Solimene, M. A. Maisto and R. Pierri, "Inverse scattering in the presence of a reflecting plane", *Journal of Optics*, vol. 18 , no. 2, 025603, 2015.

[2] R. Solimene, A. Brancaccio, J. Romano, and R. Pierri, "Localizing thin metallic cylinders by a 2.5-D linear distributional approach: Experimental results" *IEEE transactions on antennas and propagation*, vol. 56, no. 8, pp. 2630-2637, 2008.

[3] G. Ruvio, R. Solimene, A. D'Alterio, M.J. Ammann, R. Pierri "RF breast cancer detection employing a noncharacterized vivaldi antenna and a MUSIC-inspired algorithm", *International Journal of RF and Microwave ComputerâĂŘAided Engineering*, vol. 23, no. 5, pp. 598-609, 2013.

[4] R. Solimene, A. Brancaccio, R. Pierri and F. Soldovieri, "TWI experimental results by a linear inverse scattering approach", *Progress In Electromagnetics Research*, vol. 91, pp. 259-272, 2009.

[5] F. Ahmad, Y. Zhang, and M. G. Amin, "Three-dimensional wideband beamforming for imaging through a single wall," *IEEE Geosci. Remote Sens. Lett.*, vol. 5, no. 2, pp. 176âĂŞ179, 2008.

[6] F. Ahmad, M. G. Amin and S. A. Kassam, "Synthetic aperture beamformer for imaging through a dielectric wall" *IEEE Transactions on Aerospace and Electronic Systems*, vol. 41, no. 1, pp. 271-283, 2005.

[7] D. Oloumi and K. Rambabu, "Metal-cased oil well inspection using near-field UWB radar imaging," *IEEE Trans. Geosci. Remote Sens.*, vol. 56, no. 10, pp. 5884âĂŞ5892, 2018.

[8] L.-P. Song, C. Yu, and Q. H. Liu, "Through-wall imaging (TWI) by radar: 2-D tomographic results and analyses," *IEEE Trans. Geosci. Remote Sens.*, vol. 43, no. 12, pp. 2793âĂŞ2798, 2005.

[9] W. Zhang and A. Hoorfar, "Three-dimensional real-time through-thewall radar imaging with diffraction tomographic algorithm," *IEEE Trans. Geosci. Remote Sens.*, vol. 51, no. 7, pp. 4155âĂŞ4163, 2013.

[10] A. Salehi-Barzegar, A. Cheldavi, V. Nayyeri, and A. Abdolali, "A fast diffraction tomography algorithm for 3-D Through-the- Wall radar imaging using nonuniform fast Fourier transform," *IEEE Geosci. Remote Sens. Lett.*, vol. 19, pp. 1-5, 2022.

[11] F. Ahmad and M. G. Amin, "A noncoherent approach to radar localization through unknown walls," *Proc. IEEE Conf. Radar*, pp. 7, 2006.

[12] R. Solimene, M. A. Maisto, G. Romeo, R. Pierri, "On the Singular Spectrum of the Radiation Operator for Multiple and Extended Observation Domains", *International Journal of Antennas and Propagation*, vol. 2013, Article ID 585238, 10 pages, 2013

[13] M. A. Maisto, R. Solimene, and R. Pierri, "Metric entropy in linear inverse scattering" *Advanced Electromagnetics* vol. 5, no 2, pp. 46-52, 2016.

[14] M. A. Maisto, R. Pierri and R. Solimene, "Spatial Sampling in Monostatic Radar Imaging," *IEEE Geoscience and Remote Sensing Letters,* vol. 19, pp. 1-5, Art no. 3501005, 2022.

[15] M. A. Maisto, R. Pierri and R. Solimene, "Sensor Arrangement in Monostatic Subsurface Radar Imaging," *IEEE Open Journal of Antennas and Propagation,* vol. 2, pp. 3-13, 2021.